Available online at www.sciencedirect.com
SCIENCE DIRECT®
Applied Surface Science 210 (2003) 262–273
applied surface science
www.elsevier.com/locate/apsusc

Comparison of nanosecond laser ablation at 1064 and 308 nm wavelength

L. Torrisi[a,b], S. Gammino[b], L. Andò[b], V. Nassisi[c,d], D. Doria[c], A. Pedone[c,d,*]

[a]*Dipartimento di Fisica di Messina, 98128 Messina, Italy*
[b]*INFN-Laboratori Nazionali del Sud (LNS), 95124 Catania, Italy*
[c]*Dipartimento di Fisica di Lecce, Laboratorio di Elettronica Applicata (LEA), 73100 Lecce, Italy*
[d]*INFN sez. di Lecce, 73100 Lecce, Italy*

Received 16 October 2002; received in revised form 5 December 2002; accepted 5 December 2002

Abstract

To study the solid Cu ablation in vacuum, two different laser sources operating at 1064 and 308 nm wavelength are employed at similar values of laser fluences. The infrared laser is a Q-switched Nd:Yag having 9 ns pulse width (INFN-LNS, Catania), while the ultraviolet one is a XeCl excimer having 20 ns pulse width (INFN-LEA, Lecce). Both experiments produced a narrow angular distribution of the ejected material along the normal to the target surface. The ablation showed a threshold laser power density, of about 7 and 3 J/cm^2 at 1064 and 308 nm, respectively, below which the ablation effect was negligible. The laser interaction produces a plasma at the target surface, which expands very fast in the vacuum chamber. Time-of-flight (TOF) measurements of the ion emission indicated an average ion velocity of the order of 4.7×10^4 and 2.3×10^4 m/s for the infrared and ultraviolet radiation, respectively. We also estimated approximately the corresponding temperature of the plasma from which ions originated, i.e. about 10^6 and 10^5 K for IR and UV wavelength, respectively. A discussion of the analysis of the ablation mechanism is presented. At the used laser power densities the produced Cu ions showed ionisation states between 1+ and 5+ in both cases.

Keywords: Pulsed laser irradiation; Laser plasma; Time of flight; Ion beam

1. Introduction

Pulsed laser irradiation (PLI) of solid targets is a technique in fast expansion since the 1980s, featuring a wide application in different fields, such as nuclear physics, microelectronics, engineering and bio-medicine. It can be used, for example, to produce high temperature plasmas, to generate ion beams or to produce electron beams, to deposit thin biocompatible films on different substrates, and to investigate about the complex phenomena occurring in non-equilibrium plasmas [1–5].

In this work, the PLI technique is devoted to the ion generation owing to its high potentiality in generating good quality ion beams for high energy accelerators, by means of the coupling to the electron cyclotron resonant ion source (ECRIS) [6]. In this direction, PLI can be further developed to enhance the ablation rates, the plasma fractional ionisation and the production of high ion charge states.

* Corresponding author. Tel.: +39-0832-320-482; fax: +39-0832-320-505.
E-mail address: alessandro.pedone@leinfn.it (A. Pedone).

0169-4332/03/$ – see front matter
doi:10.1016/S0169-4332(02)01467-8

The coupling mechanism of the laser light to the target sample is an important key to understand the ablation phenomena. Many investigations are devoted to study the plasma characteristics as a function of the laser irradiation ones (wavelength, pulse width, pulse energy density, etc.) and to measure the maximum ion charge state produced in the non-stable expanding plasma.

Time-of-flight (TOF) measurements are particularly interesting for the investigation of the plasma plume composition because of its capability to record a complete mass spectrum at each laser shot and to evaluate the average ion kinetic energies and the plasma temperature. This allows to monitor the plasma fluctuations and temporal evolution of all the species simultaneously emitted.

The comparison of PLI of solid copper targets at two different wavelengths, in the infrared and ultraviolet regions, is presented in this paper because very interesting from the point of view of the basic involved physics. The employed lasers, operating in nearly similar experimental conditions, produce different ablation effects due to a different photon–electron energy transfer.

2. Materials and methods

Two lasers were employed for these experiments:

1. The Q-switched Nd:YAG laser at the INFN-LNS of Catania. It has a wavelength of 1064 nm, a pulse width of 9 ns (FWHM), a pulse energy ranging between 1 and 900 mJ. Laser is operated in single shot mode or in repetition mode (30 Hz). It is focused on a Cu target placed in a vacuum chamber at 10^{-7} mbar. The focusing lens has a focal length of 50 cm. The incidence angle of the beam was 45° producing a spot size of 6 mm^2 (this large spot size permitted to compare the pulse power density to the one provided by the XeCl laser).
2. The excimer XeCl laser at the INFN-LEA of Lecce. It has a wavelength of 308 nm, a pulse width of 20 ns (FWHM), and a pulse energy ranging between 1 and 100 mJ. Laser operates at a single shot and it is focused on a Cu target placed in a vacuum chamber at 10^{-6} mbar. The focusing lens has a focal length of 50 cm. The incidence angle of the radiation was 70° and the spot size on the target was 0.5 mm^2.

The experimental configurations of Catania and Lecce are very similar and their sketches are shown in Fig. 1a and b, respectively.

Similar copper targets, as a sheet of 1 cm^2 surface and 0.5 mm thickness, were employed in the two laboratories. During the experiments the target holder was connected to the ground in order to avoid stray potentials and it was rotated (10 turns/min) to irradiate a fresh surface when a high repetition rate laser beam was used.

The angular distribution of the material ejected is an important characteristic, either to get a correct beam diagnostic or to improve the coupling between the laser ion source (LIS) and the accelerators. It was monitored in both cases and evaluated by two different analysis.

(a) For the IR radiation experiment, different aluminium substrates were placed at different angles around the target so that, during the ablation process, a thin copper film was deposited on their surface at a laser fluence of 10 J/cm^2. The thin film thickness, as a function of the deposition angle, was measured through the X-ray fluorescence yield induced by 20 keV electron beam of a SEM microscope.
(b) For the UV experiment, a glass substrate was placed at about 3 cm from the target, in order to evaluate the angular distribution of ejected particle by optical measurements. By fixing the laser fluence at 10 J/cm^2, the film thickness distribution was determined measuring its optical transparency to a He–Ne laser source. The thickness profile was measured trough a 0.2 mm pinhole placed in front of the detector. The input (I_{in}) and output (I_{out}) intensities are linked by the well-known absorption relation ($I_{out} = I_{in}\, e^{-\alpha x}$, where x is the film thickness and $\alpha = 6.85 \times 10^5$ cm^{-1} is the absorption coefficient of copper at the He–Ne wavelength).

Measurements of ablation yields, for a fixed number of laser shots irradiation (generally from 100 to 500), were obtained for the total emission (neutrals and ions) by the weight loss of the copper targets. Instead,

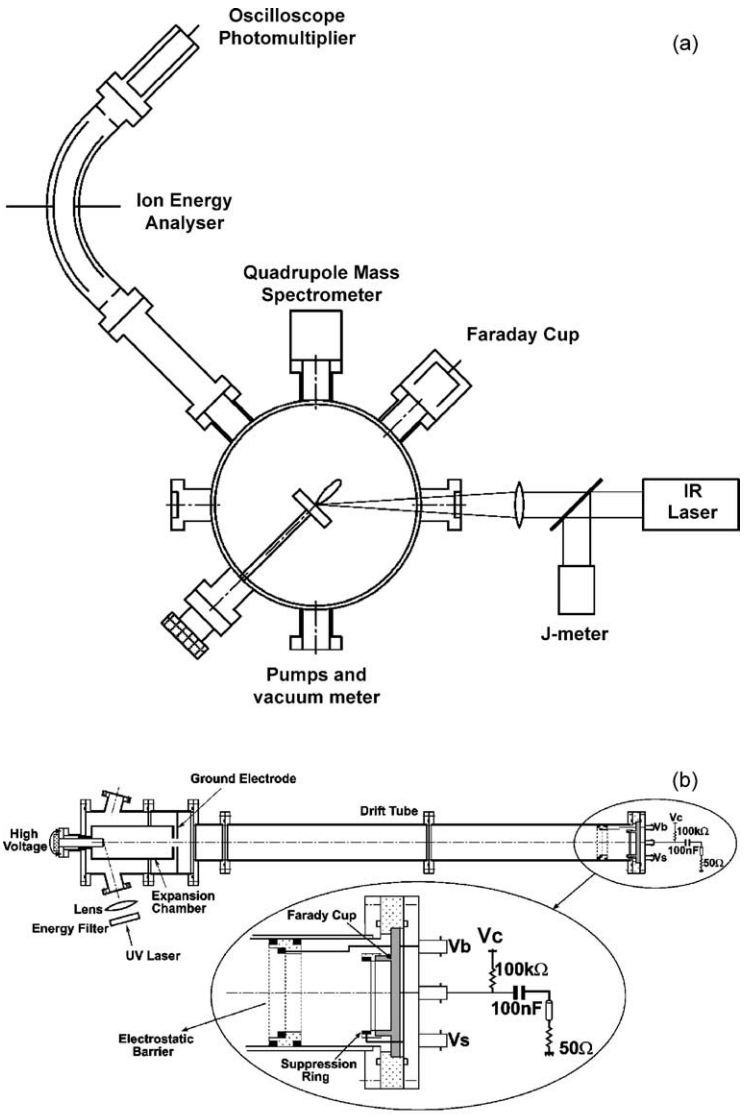

Fig. 1. Experimental set-up at LNS-Catania laboratory (a) and at LEA-Lecce laboratory (b).

for the only ion emission, current measurements were performed by using a small Faraday cup placed along the normal to the target surface.

In order to measure the plasma flux and the ion velocity, TOF measurements were performed using Faraday cups at the end of a drift tube, along the normal to the target surface. For these measurements the target-cup distance was 0.44 and 1.4 m in Catania and in Lecce laboratories, respectively. At LNS, a special ion energy analyser (IEA) having an electrostatic deflector, was also employed to measure the energy-to-charge ratio, E/q, as described in a previous work [7]. In Lecce, the ion charge states and kinetic energies were investigated placing the Faraday cup at the end of the long TOF drift tube, to increase the time resolution and to distinguish the current contribution due to different charge states, as can be seen in [8].

The deposited Cu films on substrates and the produced craters on the targets were investigated morphologically by SEM at 20 keV electron beam energy

and at different magnifications and by a high sensitively profiler (Tencor P-10) operating with 1 mg point force and 100 μm/s sweep velocity.

3. Results

By weighing the target mass before and just after a known number of laser shots, the ablation yield was determined and given in terms of removed mass (μg) of copper per laser pulse. Fig. 2 compares the copper ablation yields obtained using the two wavelengths and measuring the total mass removed per pulse by means of the laser irradiation. The results indicate that two different fluence thresholds occur at 3 and 6.7 J/cm^2 for UV and IR radiation, respectively.

As a first approximation, the different threshold values can be explained by the different irradiated volumes. In order to evaluate them, it is necessary to know the absorption depths, Z, which depends on the "skin depth", δ, and on the thermal diffusion length, L, according the following relationship [9]:

$$Z = \delta + L = \sqrt{\frac{2}{\omega\mu_0\sigma}} + \sqrt{\frac{k}{\rho c_s}\tau} \quad (1)$$

where ω is the radiation frequency, μ_0 the magnetic permeability in vacuum, σ the copper electrical conductivity, k the thermal conductivity, ρ the density, c_s the specific heat and τ the laser pulse width. Being 0.004 °C^{-1} the temperature coefficient of the copper resistivity ($1/\sigma$), at the boiling point of the copper at 10^{-7} mbar (∼1800 °C) and at the employed laser wavelengths, the electrical conductivity results 1.4×10^6 and 3.9×10^5 (Ω m)$^{-1}$ for the IR and UV radiation, respectively. In this experiment, δ is negligible with respect to L, in facts the skin depth is about 25 nm for both IR and UV, while the thermal diffusion length is 1.4 and 2.2 μm in the two cases, respectively.

By considering the spot sizes, S_0, due to the employed lasers, the irradiated mass, m, will be given by:

$$m = \rho S_0 Z \quad (2)$$

Taking into account the above parameters, the calculated mass m is 78 and 10 μg at 1064 and 308 nm, respectively.

Now, in order to coarsely justify the experimental laser fluence threshold, its theoretical value, D_{th}, can be calculated approximately through the classic

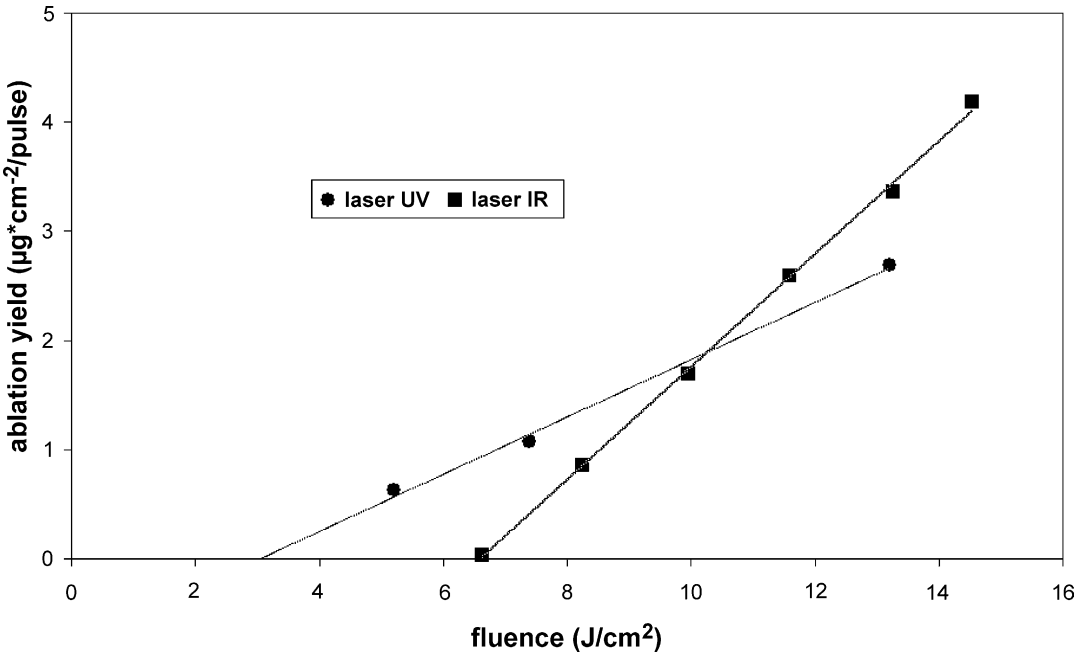

Fig. 2. Ablation yield for the total emission as a function of the laser fluence at the investigated wavelengths.

energy balance equation [10]:

$$D_{th} = \frac{m}{S_0} \times \frac{c_s \Delta T + \lambda_f + \varepsilon\lambda_e}{1 - R} \quad (3)$$

where ΔT is the temperature rise (boiling point at the chamber vacuum), c_s the specific heat, ε represents the ratio of the boiling mass on the total irradiated mass, R the reflectivity at the boiling point and, λ_f and λ_e the latent heats of fusion and evaporation, respectively.

In order to compare the theoretical threshold values to the experimental ones, it is needed to consider the absorption of the laser light in the irradiated target (factor $1 - R$). The absorption depends mainly on two factors: the target reflectivity and the plasma absorption. The latter can be neglected at the threshold conditions while the first component can be easily calculated by using the following relationship [9]:

$$R = 1 - \sqrt{\frac{8\omega\varepsilon_0}{\sigma}} \quad (4)$$

were ε_0 is the dielectric constant in vacuum. It results 0.14 and about 0 for the IR and UV radiation, respectively, using the copper electrical conductivity at the two employed wavelengths. Assuming $\varepsilon = 0$ at threshold conditions, the theoretical calculations of Eq. (3) give the values of 5.1 and 2.3 J/cm^2 for IR and UV irradiation, respectively. Although the reflectivity value calculated through Eq. (4) is only approximated, being R strongly dependent by the conditions of the irradiated surface (roughness, liquid phase, temperature, incidence angle, etc.), the calculated threshold values are in good agreement with the experimental ones, as reported in Table 1.

Another interesting result concerns the thresholds due to the only ion emission from the irradiated target. It was obtained detecting the ion current as a function of the laser fluence by means of a Faraday cup placed along the normal to the target surface. The total charge produced from the irradiated spot was then calculated taking into account the angular distribution. The obtained results, indicating the produced charge versus the laser fluence at the two wavelengths, are reported in Fig. 3. These experimental results indicate that the ion emission has almost the same experimental thresholds measured in the total emission (neutrals and ions), that the ion emission increases linearly with the laser fluence and that the ion production by UV laser is higher with respect to the IR irradiation.

The ablation yield can be given also in terms of emitted atoms or ions per single laser pulse. At the fluence of 10 J/cm^2, for example, the measured ablation yield corresponds to 1.7×10^{16} and 1.8×10^{16}

Table 1
Comparison of many data and experimental results obtained by the ablation of copper at the two used wavelengths

	Catania	Lecce
Laser wavelength, λ (nm)	1064	308
Pulse width, τ (ns)	9	20
Maximum laser energy, E_L (mJ)	900	100
Laser spot, S_0 (mm^2)	6	0.5
Incidence angle (°)	45	70
Maximum laser fluence, F_L (J/cm^2)	15	20
Thermal diffusion length, L (μm)	1.4	2.2
Laser fluence—experimental threshold, $D_{e\text{-}th}$ (J/cm^2)	6.7	3
Laser fluence—theoretical threshold, D_{th} (J/cm^2)	5.1	2.3
Reflectivity at 1800 °C, R (%)	14	∼0
Ablation yield (at 10 J/cm^2), Y (μg/cm^2 per pulse)	1.75	1.83
Fractional ionisation at 10 J/cm^2 fluence	0.09	0.36
Angular distribution (FWHM), $\Delta\phi$	±22°	±18°
Average ion velocity, $\langle v \rangle$ (m/s)	4.7×10^4	2.3×10^4
Average kinetic ion energy, $\langle E \rangle$ (eV)	920	200
Average plasma temperature, T	$\sim 2 \times 10^6$	$\sim 4 \times 10^5$
Maximum charge state, Q	+5	+5
Cu^{1+}/Cu^{2+} ratio	1.7	15.3
Grain size, G (μm)	1–5	1–5

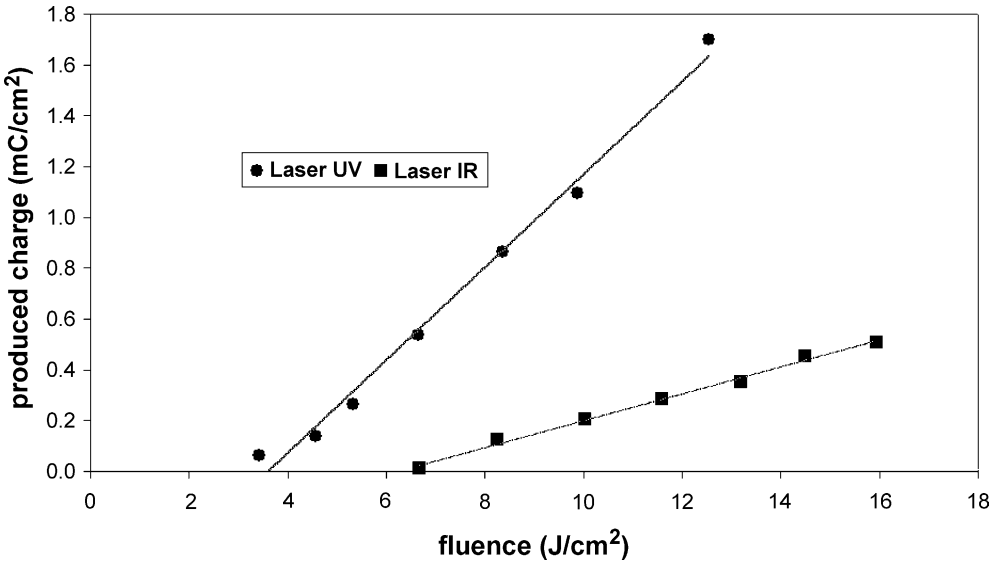

Fig. 3. Charge density of ejected ions as a function of the laser fluence at the two investigated wavelengths.

atoms/cm^2 per pulse for the total emission at 1064 and 308 nm, respectively. Assuming the ion emission to be mainly due to single charged atoms, at 10 J/cm^2 fluence the experimental ion ablation yield is about 1.6×10^{15} and 6.5×10^{15} ions/cm^2 per pulse at 1064 and 308 nm, respectively. In the above assumptions, these data permit to evaluate the fractional ionisation (ions/total ejected ratio) produced by the two laser irradiations. At 10 J/cm^2 fluence it is about 0.09 for IR ablation and 0.36 for UV ablation, a factor four higher fluence. The fractional ionisation increases suddenly at higher fluences. For example, LNS measurements performed at a fluence of 100 J/cm^2 have demonstrated that the fractional ionisation in copper increases up to about 20% [11].

The measurements of the angular distribution of the copper atoms ablated from the target are reported in Fig. 4. The data show that the angular distribution

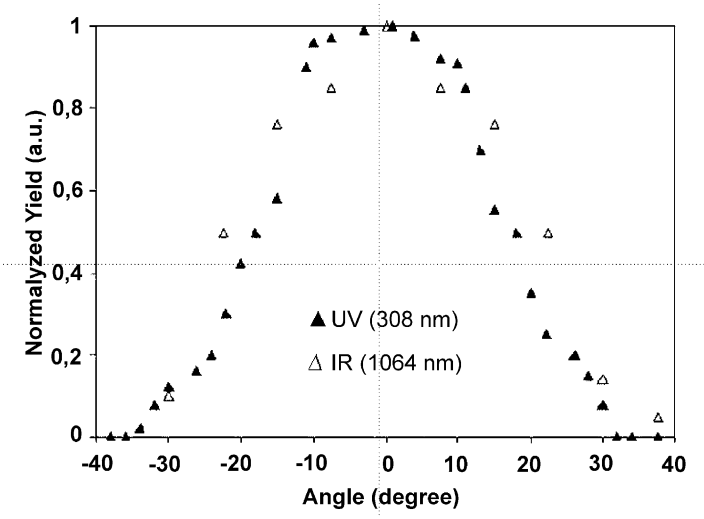

Fig. 4. Comparison of the angular distributions of ablated atoms ejected from the irradiated copper at the two wavelengths.

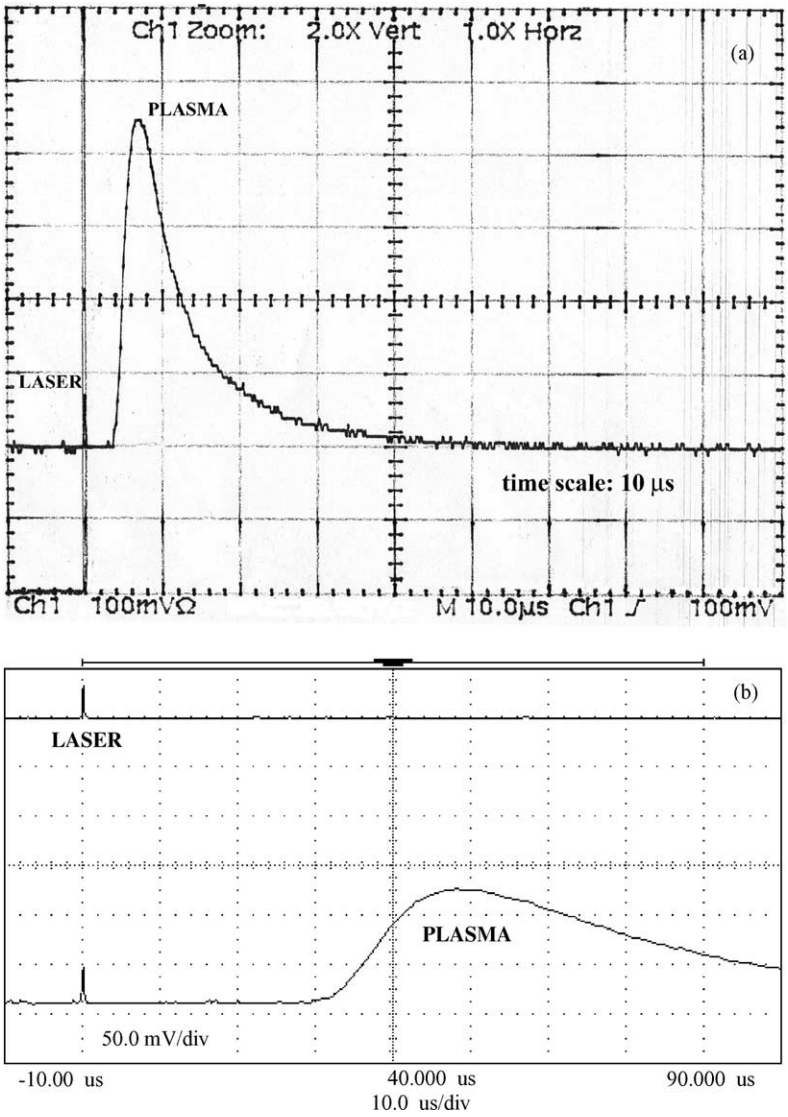

Fig. 5. Typical TOF spectrum of ion emission obtained at 1064 nm (a) and 308 nm (b).

is similar at the two used wavelengths. The emission is not isotropic, showing a symmetry around the normal direction to the target surface with a FWHM of about 44° at 1064 nm and 38° at 308 nm. This result is in good agreement with literature data [12]. These angular distributions show a flat top profile, which can be due to the self-sputtering effects of the energetic deposited atoms, according to literature [13].

Fig. 5 shows two typical TOF spectra for Cu ions obtained at LNS (a) and LEA (b) laboratory. Both spectra are detected along the normal to the target surface. Spectra show the start peak due to the laser photo-peak and a delayed large peak due to the detection of the ion component ejected from the target in the direction of the Faraday cup detector. From TOF measurements, knowing the Faraday cup-target distances, it is possible to calculate the average ion

velocities as well as the average ion energies. To do this we fitted the TOF curve with the following function [6]:

$$f(t) = [1 - e^{-(t-t_0)/\tau_1}]\, e^{-(t-t_0)/\tau_2} \quad (5)$$

where t_0 represents the minimum value of the TOF spectrum, τ_1 and τ_2 are the time constants of the rise (fast ions) and descending (slow ions) of the TOF distribution.The average velocity and kinetic energy can now be calculated as:

$$\langle v \rangle = A \int \frac{d}{t} f(t)\, dt, \qquad \langle E \rangle = A \int \frac{1}{2} m \left(\frac{d}{t}\right)^2 f(t)\, dt \quad (6)$$

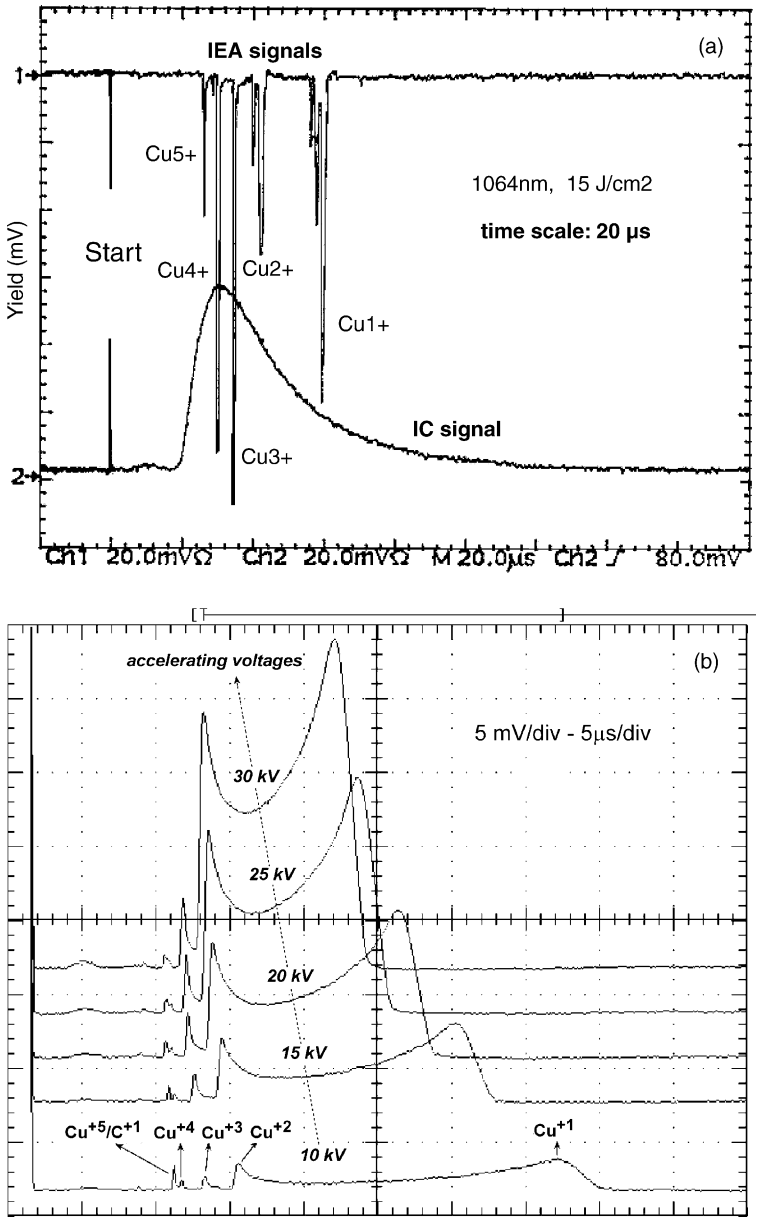

Fig. 6. Ion charge states as detected at LNS by using the IEA (b) and at INFN-LEA by using the long drift tube (b).

where A is the normalization constant. The average ion velocities result 4.7×10^4 and 2.3×10^4 m/s, respectively for 1064 nm and for 308 nm at 10 J/cm^2 fluence. Thus, the corresponding calculated average kinetic energies, $\langle E \rangle$, by Eq. (6) are 916 and 202 eV. Table 1 shows the obtained average ion velocities and kinetic energies.

The plasma produced at the target surface expands in vacuum, so its density decreases very fast so as the ion production. Assuming the expansion to be adiabatic, the plasma temperature, T, can be evaluated, according to the literature [14], by the following relationship:

$$T = \frac{\langle E \rangle}{2K_B} \left[\frac{(\gamma - 1)^2}{\gamma} \right] \tag{7}$$

where K_B is the Boltzmann constant and γ the adiabatic coefficient. This relationship is valid for a neutral emission and can be employed only as a first approximation, for ions having low charge states, in order to have an idea of the temperature value of a Boltzmann

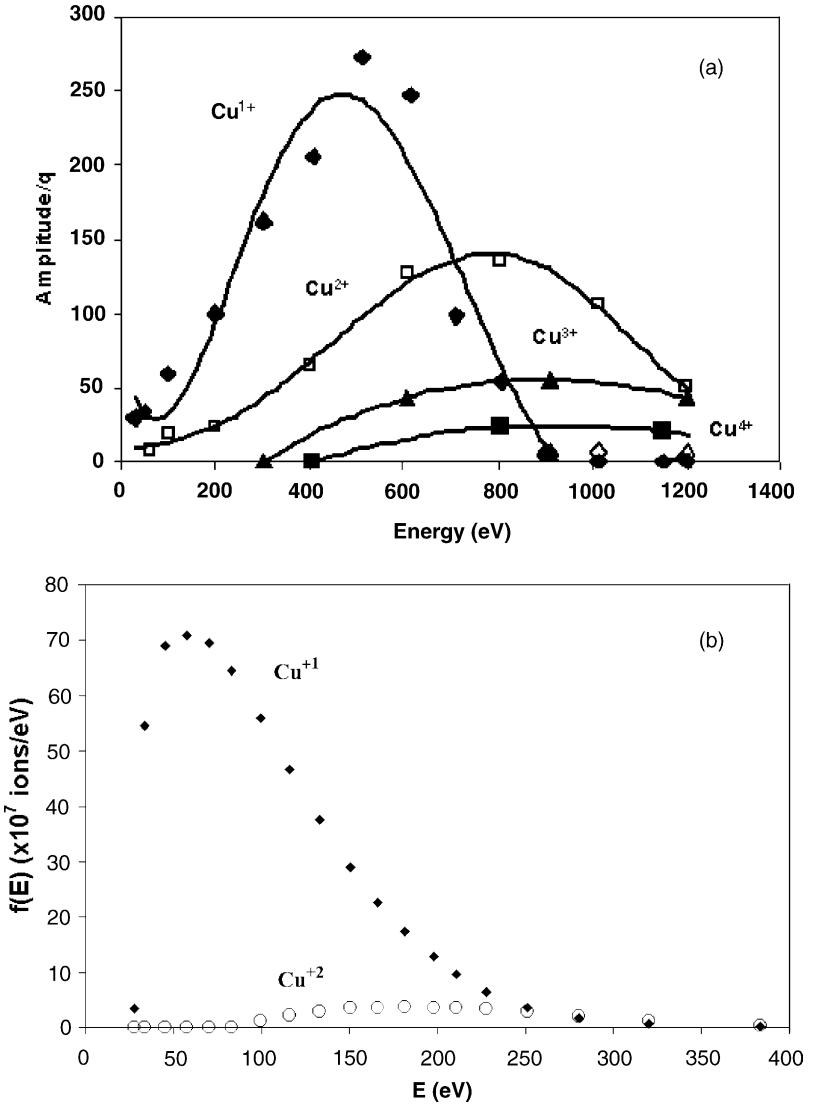

Fig. 7. Ion energy distributions for different Cu charge state due to IR (a) and UV (b) irradiation.

distributed particles. For mono-atomic species the plasma temperatures at the two-used wavelengths are of the order of 2×10^6 and 4×10^5 K, corresponding to about 170 and 34 eV, for IR and UV radiation, respectively, as reported in Table 1.

An interesting collection data concerns the ion charge state. The measurements performed in this direction using the ion energy analyser of LNS have permitted to measure both the ion energy and the ion charge state measuring the E/q ratio. Fig. 6a shows typical spectra of Cu ion detection, along the normal to the target surface, obtained at a laser fluence of 15 J/cm^2. The spectrum in the top represents the IEA detection showing five characteristic peaks due to the measure of the ion yields Cu^{1+}, Cu^{2+}, Cu^{3+}, Cu^{4+} and Cu^{5+}. The Fig. 6a shows also, for comparison, the

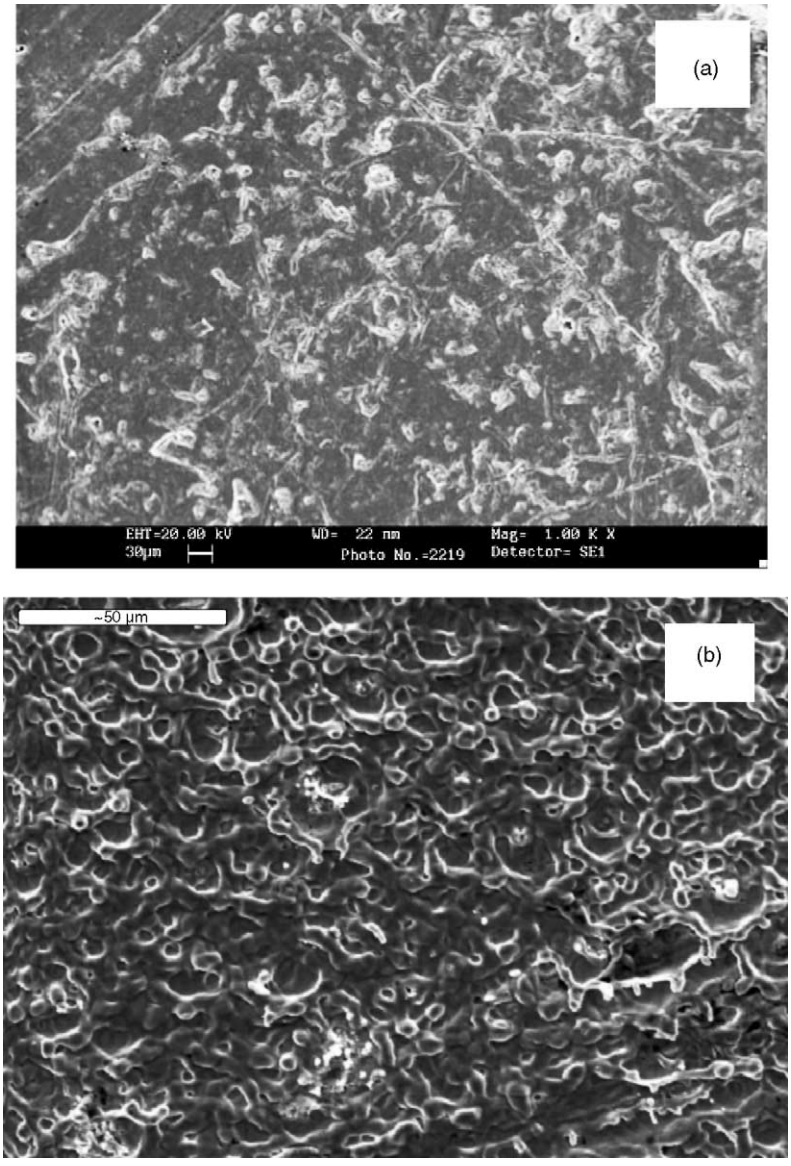

Fig. 8. Particulars of SEM investigations about the Cu films deposited on aluminium substrates at 1064 nm (a) and at 308 nm (b).

IC detection of the ions ejected by the plasma (in the bottom). Fig. 6b shows typical TOF spectra of the Cu ion detection at LEA by using different accelerating voltages, indicating a better TOF resolution at 10 kV acceleration, at which five charge states are detected.

Fig. 7a shows a typical result about the ion charge states and their energy distributions obtained at LNS by varying the electrostatic deflection bias. The distributions are approximately as a Boltzmann and show high contribution from Cu^{1+} and Cu^{2+} ions and lower contribution of the higher charge states, a result in well agreement with the literature [15].

By means of a stopping potential, as described in [7], the energy analysis of Cu^{1+} and Cu^{2+} was performed at LEA resulting in the distributions shown in Fig. 7b.

By considering the major contribution of the ion charge states, represented by Cu^{1+} and Cu^{2+}, their relative amount was evaluated by the Cu^{1+}/Cu^{2+} ratio. This relative amount is about 2 and 15 for the ion production at 1064 and 308 nm, respectively. Higher charge states are also present but with a very low intensity. Results obtained at LNS of Catania demonstrated that the ions having higher charge states have higher kinetic energy and their energy distribution is similar to a ''Boltzmann-shifted-Coulomb'' distribution [16]. Ion emission is subjected not only to the thermal and expansive velocity, such as for neutrals, but also to a Coulomb velocity due to electrical interaction between ions and target, i.e. to a residual electrical potential that produces increasing of the ions energy depending on their charge state. Thus, the total kinetic ion energy increases with the ion charge state, an effect which enlarges the ion charge distributions of the ions at higher charge states [16].

The ablated mass from the target, deposited on near aluminium substrates placed at different angle around the target, has been investigated morphologically by SEM. The thin films have been investigated in thickness and grain size distribution. Fig. 8 shows typical SEM investigations of thin Cu films deposited by using pulse laser deposition at 1064 nm (a), on Al substrate and at 308 nm (b) on glass substrate. Both films show an uniform background, probably due to the Cu evaporation process, surmounted by small grains. The average grain size is comparable for the two wavelengths and of the order of 1–5 μm. Preliminary results indicate a grain size increasing with the laser fluence. The grain size angular distribution points out a grain decreasing from the normal to the target surface towards large angles, in agreement with a previous work [12].

4. Discussions and conclusion

By comparing the results of copper ablation at 1064 and 308 nm, it is possible to observe that, although the laser power densities are comparable in the two cases and the ablation rates are similar, the average kinetic ion energy is higher for the infrared radiation with respect to the ultraviolet one. This means that also the plasma temperature is higher at 1064 nm. However, the result concerning the fractional ionisation indicates that the UV photons are more efficient to ionise the copper atoms.

The higher ion kinetic energy for infrared radiation is in agreement with the higher energy transfer, from the photons to the free electrons, determining a higher energy absorption at 1.17 eV against the 4 eV for the UV radiation. Due to the very fast laser energy deposition of the infrared laser, with respect to the ultraviolet one, it could be possible, in fact, to produce a laser irradiation of the plasma at its first stage of formation, when its density is very high. In this way the photon energy transferred to the plasma electrons produces a higher plasma temperature by thermal processes. The temperature of Cu ions produced by laser ablation at 1064 nm, in facts, is significantly higher than for 308 nm, which would originate from the efficient heating of plasma by inverse Bremsstrahlung absorption at 1064 nm [17].

The angle distribution of the atomic emission around the normal to the target surface is practically the same for both radiations at the same fluence. Results indicate a larger distribution using the IR radiation, due to the larger thermal effect (evaporation component), in agreement with the literature [14].

The grain size distribution in the deposited films is similar for both radiations at the same fluence. The micrometric grains in both cases can be justified by the non-equilibrium phenomena which can generate clusters emission and splashing effects with a production of micro-metric grains in the deposited film [10].

Acknowledgements

The authors are pleased to acknowledge the excellent technical assistance during laser irradiation of Mr. C. Percolla of the INFN-LNS of Catania and of V. Nicolardi of the INFN-LEA of Lecce. The financial support of the Fifth National Committee of INFN given to this work through the ECLISSE and SOLAI Projects is gratefully acknowledged.

References

[1] D.H.H. Hoffmann et al., Nucl. Instrum. Meth. Phys. Res. B 161–163 (2000) 9–18.
[2] L. Torrisi, S. Trusso, G. Di Marco, P. Parisi, Phys. Med. XVII (4) (2001) 227.
[3] W. Mroz et al., Rev. Sci. Instrum. 65 (1994) 1272.
[4] V. Nassisi, V. Stagno, J. Appl. Phys. 76 (1994) 3769.
[5] D.B. Chrisey, G.K. Hubler, in: D.B. Chrisey, G.K. Hubler (Eds.), Pulsed Laser Deposition of Thin Films, Wiley, New York, 1994.
[6] S. Gammino et al., Rev. Sci. Instrum. 71 (2000) 1119.
[7] S. Gammino, et al., The Eclisse Experiment: Production of High Intensity Ion Beam by Means of a Hybrid Ion Source, Report INFN-LNS, IFN/TC 02, SIS Publ. LNF, 22 February 2002.
[8] V. Nassisi, A. Pedone, A. Rainò, Nucl. Instrum. Meth. B 188 (2002) 267–271.
[9] G. Bekefi, A.H. Barrett, Electromagnetic Vibrations, Waves and Radiations, Massachusetts Institute of Technology, 1977.
[10] L. Torrisi, G. Ciavola, S. Gammino, L. Andò, A. Barnà, L. Laska, J. Krasa, Rev. Sci. Instrum. 71 (2000) 4330.
[11] L. Torrisi, L. Andò, S. Gammino, J. Krasa, L. Laska, . Nucl. Instrum. Meth. Phys. Res. B 184 (2001) 327.
[12] L. Torrisi, L. Andò, G. Ciavola, A. Barnà, Rev. Sci. Instrum. 72 (2001) 68.
[13] H.U. Krebs, O. Bremert, Appl. Phys. Lett. 62 (19) (1993) 2341.
[14] D.B. Geohegan, Diagnostic and characteristics of pulsed laser deposition laser plasmas from pulsed laser deposition of thin films, in: D.B. Chrisey, G.K. Hubler (Eds.), Wiley, New York, 1994, p. 115, Chapter 5.
[15] J. Hasegawa, M. Yoshida, Y. Oguri, M. Ogawa, M. Nakajima, K. Horioka, Nucl. Instrum. Meth. B 161–163 (2000) 1104.
[16] L. Torrisi, L. Andò, S. Gammino, L. Laska, J. Appl. Phys. 91 (2002) 18.
[17] J.Y. Moon, S.M. Park, Bull. Korean Chem. Soc. 20 (9) (1999) 1101.